

# Superradiant phase transition in a large interacting driven atomic ensemble in free space

Janne Ruostekoski

Department of Physics, Lancaster University, Lancaster, LA1 4YB, United Kingdom

(Dated: May 2, 2024)

Atomic ensembles strongly interacting with light constitute rich quantum-optical many-body systems, with the potential for observing cooperative effects and dissipative nonequilibrium phase transitions. We theoretically analyze the conditions under which a driven atomic ensemble in free space, characterized by strong dipole-dipole interactions and large spatial extent, can undergo a superradiant phase transition, also known as cooperative resonance fluorescence. In an atomic array, stationary states that conserve the collective pseudospin exhibit completely cooperative decay and undergo a second-order phase transition in the large atom number limit. In contrast, decay mechanisms on longer timescales that fail to conserve pseudospin can lead to discontinuous first-order phase transition at a critical finite atom number, disrupting cooperation despite sharing many similar observable characteristics. A hallmark of the superradiant phase transition is an abrupt shift from total light reflection off the atoms to rapidly increasing transmission, accompanied by significant quantum fluctuations, as a function of light intensity.

## I. INTRODUCTION

Recent years have seen a dramatic resurgence in interest in collective optical interactions between atoms, stimulated by enhanced experimental imaging capabilities of cold atoms at high densities [1–10]. This has renewed focus on foundational models of cooperative phenomena, such as the Dicke model [11] for superradiance [12–25]. While the emission in Dicke superradiance, with the intensity proportional to the square of the atom number  $N^2$ , is essentially a classical effect of phased dipoles, its extension to a driven case—*cooperative resonance fluorescence* (CRF)—reveals intricate quantum behaviors and phase transition phenomena [26–33]. In CRF, an idealized system of noninteracting two-level atoms are confined to volume smaller than a cubed resonant wavelength, such that their identical response to light can be represented by a collective pseudospin operator  $\hat{S}_\pm = \sum_j \hat{\sigma}_j^\pm$  and  $\hat{S}_z = \sum_j \hat{\sigma}_j^z$ , with  $\hat{S}_\pm = \hat{S}_x \pm i\hat{S}_y$ , where  $\hat{\sigma}_j^+ = |e\rangle\langle g|$  is the raising spin operator for atom  $j$ . This configuration conserves the total pseudospin  $\langle \hat{S}^2 \rangle$ , or the radius of the Bloch sphere, and decays through a completely cooperative mechanism, which in less idealized scenarios is limited by short coherence times. The CRF supports two nonequilibrium phases: At weak driving, fluorescence is classical from an induced collective dipole that attenuates the incident field. At high intensities, the system undergoes a second-order phase transition where, in the limit  $N \rightarrow \infty$ , the excited level sharply saturates, the mean dipole moment vanishes, and quantum fluctuations increase significantly.

Inspired by a recent experimental report on the observation of the superradiant phase transition [34], traditionally referred to as CRF, in a dilute atom cloud in free space, we develop a simple and tractable theoretical model to explore this phase transition within a spatially extended atomic ensemble experiencing strong dipole-dipole (DD) interactions in free space. We dis-

cover that, in a planar array of closely spaced atoms in a superradiant mode with a broad resonance linewidth, the system can conserve a macroscopic pseudospin on short timescales, leading to complete cooperative decay and a second-order phase transition. A hallmark of this phase transition is an abrupt shift in the array’s properties from a perfect mirror to rapidly increasing light transmission, accompanied by enhanced quantum fluctuations. Both the transition point and the scattered light intensity depend on the self-interaction resonance linewidth leading to different scaling with the atom number compared with the idealized noninteracting system confined to volume with dimensions much smaller than a wavelength. The counterintuitive result that strong DD interactions enable CRF can be attributed to delocalized excitations that, paradoxically, enhance the indistinguishability of the atoms.

When the pseudospin is not conserved, the behavior of single-atom observables at large atom numbers can still, surprisingly, approximate the sharp functional dependence typical of CRF. At high densities, the decay mechanism that fails to conserve the pseudospin may instead undergo a first-order phase transition at a critical atom number, indicative of optical bistability [35–41]. We demonstrate that sufficiently weak position fluctuations do not prevent bistability, and how even stronger fluctuations can still preserve other distinct characteristics of single-atom observables. Independently to our work, the CRF experiment [34] is theoretically analyzed in Refs. [42, 43].

## II. ATOM-LIGHT INTERACTIONS

We study  $N$  two-level atoms in a 2D square array with lattice constant  $a$  and unit filling. Light mediates strong DD interactions through multiple scattering. The quantum-optical properties of such planar arrays have recently been reviewed in Ref. [44]. We first analyze the

atomic coherences  $\rho_{ge}^{(j)} = \langle \hat{\sigma}_j^- \rangle$  and the excited level populations  $\rho_{ee}^{(j)}$  of atom  $j$  at  $\mathbf{r}_j$  employing the semiclassical approximation where quantum fluctuations between different atoms [45] are ignored (the ground state populations are derived from  $\rho_{gg}^{(j)} = 1 - \rho_{ee}^{(j)}$ ). The dynamics in the rotating-wave approximation are then given by

$$\dot{\rho}_{ge}^{(j)} = (i\Delta - \gamma)\rho_{ge}^{(j)} - i(2\rho_{ee}^{(j)} - 1)\mathcal{R}_{\text{eff}}^{(j)}, \quad (1a)$$

$$\dot{\rho}_{ee}^{(j)} = -2\gamma\rho_{ee}^{(j)} + 2\text{Im}[(\mathcal{R}_{\text{eff}}^{(j)})^* \rho_{ge}^{(j)}], \quad (1b)$$

where  $\gamma = \mathcal{D}^2 k^3 / (6\pi\hbar\epsilon_0)$  is the single-atom resonance linewidth,  $\mathcal{D}$  the dipole matrix element, with the atomic dipole  $\mathbf{d} = \mathcal{D}\hat{\mathbf{e}}_d$ , and  $k = 2\pi/\lambda$  the resonance wavenumber. Effective Rabi frequencies [46],

$$\mathcal{R}_{\text{eff}}^{(j)} = \mathcal{R}^{(j)} + \xi \sum_{\ell \neq j} \mathbf{G}_{dd}^{(j\ell)} \rho_{ge}^{(\ell)}, \quad \xi = \frac{\mathcal{D}^2}{\hbar\epsilon_0}, \quad (2)$$

drive atom  $j$  and include the contributions from the incident field Rabi frequency  $\mathcal{R}^{(j)} = \mathcal{D}\hat{\mathbf{e}}_d \cdot \mathcal{E}^+(\mathbf{r}_j)/\hbar$  and from the scattered fields from all the other atoms at  $\mathbf{r}_\ell$  through the dipole radiation kernel  $\mathbf{G}(\mathbf{r})$  [47]

$$\mathbf{G}_{\nu\mu}(\mathbf{r}) = \left[ \frac{\partial}{\partial r_\nu} \frac{\partial}{\partial r_\mu} - \delta_{\nu\mu} \nabla^2 \right] \frac{e^{ikr}}{4\pi r} - \delta_{\nu\mu} \delta(\mathbf{r}) \quad (3)$$

in  $\mathbf{G}_{dd}^{(j\ell)} = \hat{\mathbf{e}}_d^* \cdot \mathbf{G}(\mathbf{r}_j - \mathbf{r}_\ell) \hat{\mathbf{e}}_d$ . The positive frequency component of the light amplitude  $\mathcal{E}^+(\mathbf{r}_j)$  and  $\rho_{ge}^{(j)}$  are expressed as slowly varying amplitudes where the rapid oscillations at the laser frequency have been factored out. The second term in Eq. (2) can induce recurrent scattering and strong DD interactions. Omitting this term results in the standard optical Bloch equations. The semiclassical theory of Eq. (1) for planar arrays was found in Ref. [45] to agree well with the quantum solution, particularly when exciting collective modes with broad superradiant resonances, as we consider here. However, quantum effects are crucial in the dynamics of phase transitions.

We now develop a simple model to describe the steady states of Eqs. (1) and (2). Assuming phase-uniform incoming light that is normally incident to the array, we treat each atom as equally driven, with  $\mathcal{R}^{(j)} = \mathcal{R}$ . We disregard edge effects, an approximation that becomes accurate for large arrays. We concentrate on stable steady states with a uniform phase profile that directly couple to the incident light. Consequently, we set  $\rho_{ee}^{(j)} = \rho_{ee}$  and  $\rho_{ge}^{(j)} = \rho_{ge}$ , resulting in uniform  $\mathcal{R}_{\text{eff}} = \mathcal{R} + \rho_{ge} \xi \sum_{\ell \neq j} \mathbf{G}_{dd}^{(j\ell)} = \mathcal{R} + (\tilde{\Omega} + i\tilde{\gamma})\rho_{ge}$ , where  $\tilde{\Omega}$  and  $\tilde{\gamma}$  represent the real and imaginary components, respectively, of the radiation kernel  $\tilde{\Omega} + i\tilde{\gamma} = \xi \sum_{\ell \neq j} \mathbf{G}_{dd}^{(j\ell)}$  [46]. In the absence of edge effects, the lattice is considered translationally invariant, rendering the position of site  $j$  arbitrary. The steady-state solutions of Eq. (1) now read

$$\rho_{ge} = \mathcal{R}_{\text{eff}} \frac{-\Delta + i\gamma}{\Delta^2 + \gamma^2 + 2|\mathcal{R}_{\text{eff}}|^2}, \quad (4a)$$

$$\rho_{ee} = \frac{|\mathcal{R}_{\text{eff}}|^2}{\Delta^2 + \gamma^2 + 2|\mathcal{R}_{\text{eff}}|^2}. \quad (4b)$$

Analogous uniform excitations were also observed experimentally in the transmission of light through an atomic planar array, conducted in the low light intensity (LLI) limit in Ref. [8]. In practise, possessing a large array size is not essential for the effectiveness of the approximation Eq. (4); it suffices that the phase profiles are uniform. In finite arrays, the coupling to phase-uniform modes can be significantly enhanced by adjusting the width of a Gaussian laser beam to match the lattice size [48]. A detailed analysis of mode matching errors was carried out in Ref. [49].

Using Eq. (4a) and the expression for  $\mathcal{R}_{\text{eff}}$ , we obtain the relationship between  $\mathcal{R}$  and  $\mathcal{R}_{\text{eff}}$  depending on the cooperativity parameter  $C = (\tilde{\Omega} + i\tilde{\gamma})/[2(\Delta + i\gamma)]$  [46],

$$\mathcal{R} = \mathcal{R}_{\text{eff}} + \mathcal{R}_{\text{eff}} \frac{2C(\Delta^2 + \gamma^2)}{\Delta^2 + \gamma^2 + 2|\mathcal{R}_{\text{eff}}|^2}. \quad (5)$$

Taking the absolute value of both sides of Eq. (5) yields a cubic equation in  $|\mathcal{R}_{\text{eff}}|^2$ , which may have one or two dynamically stable solutions—indicating optical bistability.

### A. Low light intensity excitation eigenmodes

Even beyond the LLI regime, the collective atom behavior can be described by the properties of underlying LLI collective radiative excitation eigenmodes. In the LLI limit [50], Eq. (1) simplifies to Eq. (1a) with  $\rho_{ee} = 0$ . The resulting dynamics of coupled linear dipole oscillators are expressed as:

$$\dot{\rho}_{ge}^{(j)} = i \sum_{\ell} (\mathcal{H}_{j\ell} + \delta\mathcal{H}_{j\ell}) \rho_{ge}^{(\ell)} + i\mathcal{R}^{(j)}, \quad (6)$$

where the matrix  $\delta\mathcal{H}_{j\ell}$  includes  $\Delta$  on the diagonal and

$$\mathcal{H}_{j\ell} = i\gamma\delta_{j\ell} + \xi \mathbf{G}_{dd}^{(j\ell)} (1 - \delta_{j\ell}) \quad (7)$$

provides the collective excitation eigenmodes [51, 52]. The eigenvalues  $\delta_j + iv_j$  yield the LLI collective line shift  $\delta_j$  and collective linewidth  $v_j$ . For the uniform LLI eigenmode, the eigenvalue  $\eta$  satisfies [44]  $\mathcal{H}\rho_{ge} = \eta\rho_{ge}$ , or

$$\mathcal{H}\rho_{ge} = (i\gamma + \xi \sum_{\ell \neq j} \mathbf{G}_{dd}^{(j\ell)}) \rho_{ge} = [\tilde{\Omega} + i(\gamma + \tilde{\gamma})] \rho_{ge}, \quad (8)$$

with the line shift  $\tilde{\Omega}$  and linewidth  $v = \gamma + \tilde{\gamma}$ . Both  $\tilde{\Omega}$  and  $\tilde{\gamma}$  can be numerically calculated for finite arrays. These parameters critically influence the behavior of the effective field  $\mathcal{R}_{\text{eff}}$  in Eq. (5) through the cooperativity parameter  $C$ .

## B. Collective $\langle \hat{S}_z \rangle$ breaking interactions

Next we solve Eq. (1) for varying atom numbers  $N$  by solving the cubic equation for  $|\mathcal{R}_{\text{eff}}|^2$  derived from Eq. (5). The dependence on  $N$  arises through the cooperativity parameter  $C$ , obtained by numerically calculating  $\tilde{\Omega}(N)$  and  $\tilde{\gamma}(N)$  for different  $N$ . In Fig. 1, we show  $s_z = 2\rho_{ee} - 1$  and  $|\mathcal{R}_{\text{eff}}|$  for lattice spacings  $a/\lambda = 0.17$  and  $0.16$ , and examples of  $\tilde{\gamma}$  as a function of  $N$  are displayed in Fig. 2(a). As  $N$  increases,  $s_z$  develops a more pronounced concave curve, reaching a sharp inflection point near saturation—traits also characteristic of CRF. Initially, for increasing intensities, the incident light is dampened by the induced atomic polarization, resulting in weak  $|\mathcal{R}_{\text{eff}}|$ , until reaching a threshold intensity where  $|\mathcal{R}_{\text{eff}}|$  begins to increase rapidly. The sharpening of these curve profiles results from the broadening linewidth  $\gamma + \tilde{\gamma}$ . However, no phase transition occurs at  $a = 0.17\lambda$ . The scenario changes at  $a = 0.16\lambda$  where, beyond a critical atom number,  $|\mathcal{R}_{\text{eff}}|$  exhibits three solutions, indicating optical bistability and representing a discontinuous first-order phase transition. Two of the solutions are stable and the one with a negative gradient unstable. Analogous to optical cavity bistability [36], the two stable branches in Fig. 1 are referred to as cooperative (low  $s_z$ ) and single-atom (high  $s_z$ ) solutions [41]. The bistability is intrinsic, generated by DD interactions in free space in the absence of a cavity. Theoretical studies suggest that such interaction-mediated bistable behavior can be generic in cold-atom systems with a variety of short- and long-range interactions [53–55], and it has been experimentally observed in Rydberg atoms in the microwave regime [56]. Small lattice constants  $a/\lambda \simeq 0.08$  and  $0.17$  at magic wavelengths that generate strong DD interactions are achievable with Sr [57, 58] and Yb [59] atoms, respectively.

As the atom positions are encoded in the collective linewidths  $\gamma + \tilde{\gamma}$  and line shifts  $\tilde{\Omega}$ , we examine the impact of weak position fluctuations on the phase transition by calculating the changes in  $\gamma + \tilde{\gamma}$  and  $\tilde{\Omega}$  due to disorder. We solve the coupled LLI equations for the eigensystem  $\mathcal{H}$ , randomly sampling atom positions around each lattice site from Gaussian density distributions with a root-mean-square width  $\eta$  [60]. By ensemble-averaging over many stochastic realizations, we obtain the expectation values of  $\langle \tilde{\gamma} \rangle$  and  $\langle \tilde{\Omega} \rangle$ . With sufficiently weak fluctuations, the relevant mode largely retains its phase uniformity. In deep optical lattice potentials,  $\eta$  can be related to the lattice height in terms of lattice photon recoil energies  $s$ , with  $\eta/a = s^{-1/4}/\pi$  [61]. Intriguingly, as demonstrated in Fig. 2, while bistability persists under weak fluctuations, stronger fluctuations may eliminate bistability yet preserve the sharp features of the  $s_z$  curve, reminiscent of CRF.

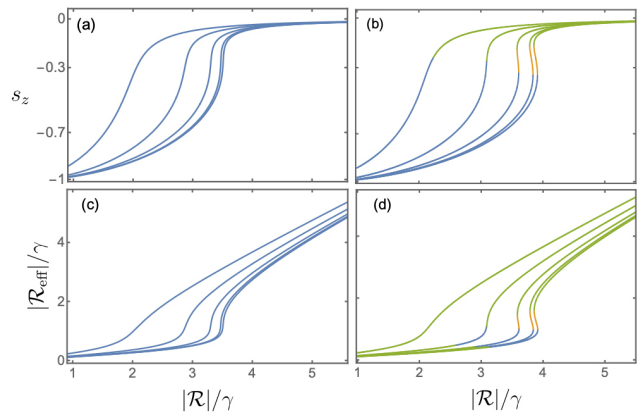


Figure 1. The atom number  $N$  dependence of (a,b) the collective atomic pseudospin component  $s_z$  and (c,d) the effective Rabi frequency  $|\mathcal{R}_{\text{eff}}|$  driving each atom in the array as a function of the Rabi frequency of the incident driving  $|\mathcal{R}|$  for lattice constants (a,c)  $a/\lambda = 0.17$  and (b,d)  $0.16$ . The curves from top to bottom  $N = 4, 9, 16, 25, 36$  reaching the asymptotic large  $N$  value. (b,d) First-order phase transition and optical bistability above a critical  $N$  are observable in the last three curves; (a,c) no phase transition.

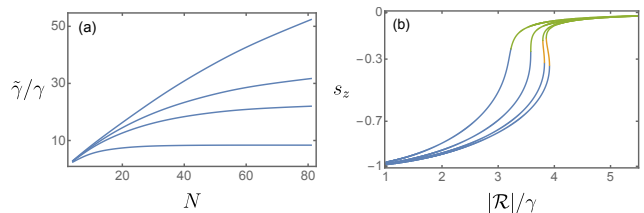


Figure 2. (a) The atom number  $N$  dependence of the collective self-interaction linewidth  $\tilde{\gamma}$ . The curves from top to bottom for the lattice constants:  $a/\lambda = 0.05, 0.08, 0.10,$  and  $0.16$ . (b) The effect of position fluctuations of atoms on the bistability phase transition in the large  $N$  limit for  $a = 0.16\lambda$  shown in Fig. 1(b). The curves from top to bottom for the atom density root-mean-square widths  $\eta/a$  at each site:  $0.3, 0.2, 0.1,$  and  $0$ . The phase transition is observable at  $\eta/a = 0$  and  $0.1$ .

## C. Collective $\langle \hat{S}_z \rangle$ conserving interactions

As we analyze Eq. (1) for broad superradiant resonances, where the linewidths satisfy  $\nu \gg \gamma$ , we can neglect the terms proportional to  $\gamma$  for observation times shorter than  $1/\gamma$ . Consequently, we reformulate Eq. (1) for uniform excitations using scaled collective pseudospin expectation values  $s_z = 2\langle \hat{S}_z \rangle / N = 2\rho_{ee} - 1$  and  $s_- = 2\langle \hat{S}_- \rangle / N = 2\rho_{ge}$ :

$$\dot{s}_- = i\Delta s_- - is_z[2\mathcal{R} + (\tilde{\Omega} + i\tilde{\gamma})s_-], \quad (9a)$$

$$\dot{s}_z = i\mathcal{R}(s_+ - s_-) - \tilde{\gamma}|s_-|^2, \quad (9b)$$

where, without the loss generality, we have taken  $\mathcal{R}$  to be real. We discover that  $\frac{d}{dt}(s_z^2 + |s_-|^2) = 0$ , indicating that the collective pseudospin  $s^2 = s_z^2 + s_x^2 + s_y^2 \leq 1$  is conserved for the macroscopic spin  $S = N/2$ . Remarkably,

this dynamic closely mirrors the idealized CRF observed in entirely noninteracting atoms confined to a volume smaller than a cubed resonant wavelength. Analyzing the steady-state solutions where  $\dot{s}_- = \dot{s}_z = 0$  at the collective resonance  $\Delta = s_z \tilde{\Omega}$ , we derive from Eq. (9a) that either  $s_z = 0$  or  $s_- = i\beta$ , where  $\beta = 2\mathcal{R}/\tilde{\gamma}$ .

*The case  $s_- = i\beta$ :* From Eq. (9b) and the conservation equation for  $s^2$ , we derive  $s_z = -\sqrt{s^2 - \beta^2}$ , where the positive sign before the square root does not yield a stable solution. This relationship holds for  $\beta^2 \leq s^2 \leq 1$ , encompassing the weak field limit where the excited level population vanishes ( $s_z = -1$ ). As the incident light amplitude increases, the coherence  $\rho_{ge}$  rises linearly until it reaches its maximum at  $|\rho_{ge}| = |s|/2$ , corresponding to the saturation point of the excited level at  $\rho_{ee} = 1/2$  ( $s_z = 0$ ). In this scenario, the increasing induced dipole  $\rho_{ge}$  attenuates incident driving, resulting in a weak effective Rabi frequency driving each atom  $\mathcal{R}_{\text{eff}} = i\mathcal{R}\tilde{\Omega}/\tilde{\gamma}$ . Notably, at the single-atom resonance ( $\Delta = 0$ )  $\mathcal{R}_{\text{eff}} = 0$  exactly cancels out. For atomic arrays, the collective behavior can be observed in light transmission experiments, analogous to Refs. [8, 10] (see Appendix A). At the collective resonance the array acts as a perfect mirror  $r \simeq -1$ , for  $\tilde{\gamma} \gg \gamma$  [Eq. (A4)]. Intriguingly, this regime of perfect reflection spans the entire range of  $\rho_{ee}$  from zero to saturation, significantly extending the LLI observations of an atomic mirror [8].

*The case  $s_z = 0$ :* From the conservation of  $s^2$  and Eq. (9b), we derive  $s_- = is^2/\beta \pm \sqrt{s^2 - s^4/\beta^2}$  for  $\beta^2 \geq s^2$ . As  $\beta$  increases, while  $s_z = 0$  remains saturated, the magnitude of  $|\rho_{ge}|$  no longer escalates or offsets the increasing incident light, resulting in rapid growth in  $\mathcal{R}_{\text{eff}}$ . The power reflection  $|r|^2 \simeq \beta^{-2}$  begins to decrease as  $\mathcal{R}$  rises. Correspondingly, the transmission  $|t|^2 \simeq 1 - \beta^{-2}$  increases. Different factorizations can lead to different mean-field solutions. Analogous to CRF, these solutions are not stable [28]; rather, small perturbations result in periodic oscillations around the stationary state.

We can formulate an approximate quantum master equation for the density matrix  $\hat{\rho}$  by focusing only on the coupling to the phase-uniform collective mode, analogously to the approach used in Eq. (9). Assuming the collective resonance, the quantum analog of Eq. (9) reads

$$\dot{\hat{\rho}} = i[2\mathcal{R}\hat{S}_x, \hat{\rho}] + \frac{2\tilde{\gamma}}{N} \left( 2\hat{S}_- \hat{\rho} \hat{S}_+ - \hat{S}_+ \hat{S}_- \hat{\rho} - \hat{\rho} \hat{S}_+ \hat{S}_- \right), \quad (10)$$

where the bracket denotes a commutator. The relationship between Eqs. (10) and (9) is then the same as the one between the quantum and semiclassical theories of CRF of noninteracting atoms confined to volume with dimensions much smaller than a wavelength [27–33]. The single-atom linewidth  $\gamma$  of the CRF master equation is replaced in Eq. (10) by the scaled collective self-interaction linewidth of the atom array  $2\tilde{\gamma}/N$ . This modifies the dependence of the transition point on the atom number from  $N/2$  to a slower-than-linear scaling with  $\tilde{\gamma}/\gamma$  [see Fig. 2(a)]. Although the solutions to Eq. (10) have been

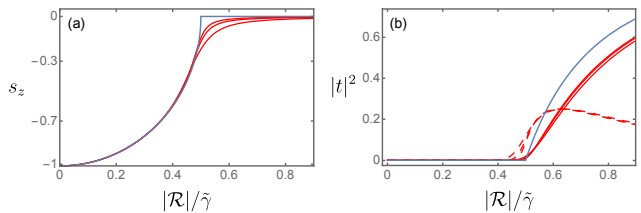


Figure 3. Cooperative resonance fluorescence. (a) The collective atomic spin  $s_z$  and (b) power transmission coefficient  $|t|^2$  for coherently scattered light through the atom array display a second-order phase transition as a function of  $\mathcal{R}$  scaled by the collective self-interaction linewidth  $\tilde{\gamma}$ . In (a), the curves from top to bottom: the semiclassical solution, quantum solutions for  $N = 80, 50$ , and  $25$ . The quantum solutions asymptotically approach the semiclassical curve with discontinuous derivative. In (b), the perfect reflection is maintained at intensities all the way to saturation point, after which the perfect array reflection sharply transitions to rising transmission. The quantum solutions (the lower solid curves) asymptotically approach a curve distinct from the semiclassical result (top curve). The quantum fluctuations derived from  $\langle s_+ s_- \rangle - |\langle s_+ \rangle|^2$  are shown in the corresponding incoherent transmission contribution (dashed line).

thoroughly explored (also for more recent results see, e.g. Ref. [62]) we can directly relate them to the power transmission coefficients  $|t|^2$  of coherently scattered light through the atomic array (Appendix A). In Fig. 3, the rescaled steady-state solutions of Eq. (10) for the spin expectation values and transmission are shown for varying  $N$  alongside the mean-field solutions of Eq. (9). Both cases converge at a critical transition point where the excited state saturates, and perfect array reflection sharply transitions to increased transmission.

For  $\langle s_z \rangle$  in Fig. 3(a), the quantum solution smoothly approaches the mean-field solution as  $N \rightarrow \infty$ , marking a clear second-order phase transition. However, the quantum solution  $\langle s_x \rangle = 0$  significantly differs from the mean-field theory [32], with discrepancies also noted for  $\langle s_y \rangle$ . These differences impact  $|t|^2$ , shown in Fig. 3(b), where the quantum solutions for increasing  $N$  asymptotically approach a curve distinct from the mean-field predictions, indicating strongly enhanced quantum fluctuations. The expression  $|\langle s_+ \rangle|^2 + \langle s_z \rangle^2$  is no longer conserved, unlike  $\langle s_+ s_- \rangle + \langle s_z^2 \rangle$  [32], as demonstrated in Fig. 3(b) by the component of incoherently transmitted light originating from  $\langle s_+ s_- \rangle - |\langle s_+ \rangle|^2$  (Appendix A). Fluctuations in light transmission are a strong signature of significant quantum effects beyond the mean-field theory.

#### D. Scattered intensity

We now examine how the scattered light intensity depends on the atom number  $N$ . From the single-atom contributions in Eqs. (4) we find that the coherent scattering due to  $\rho_{ge}$  is dominant at low intensities, whereas at high



intensities, incoherent scattering from  $\rho_{ee}$  becomes prevalent. The general expression for coherent scattering rate of photons, integrated over a closed surface enclosing the source, is given by (see Appendix A)

$$n_c = 2\gamma \sum_j \langle \hat{\sigma}_j^+ \rangle \langle \hat{\sigma}_j^- \rangle + 2\xi \sum_{j\ell(j\neq\ell)} \text{Im}[\mathbf{G}_{dd}^{(j\ell)}] \langle \hat{\sigma}_j^+ \rangle \langle \hat{\sigma}_\ell^- \rangle. \quad (11)$$

For the phase-uniform mode we directly obtain

$$n_c = 2N(\gamma + \tilde{\gamma})|\rho_{ge}|^2, \quad (12)$$

since  $\langle \hat{\sigma}_j^\pm \rangle$  can be taken outside the sum. More generally for the array, the correlations due to DD interactions alter the typical scaling from  $N^2$  to  $N\tilde{\gamma}/\gamma$  where  $\tilde{\gamma}$  initially increases with small  $N$  but quickly begins to saturate. For instance, for the lower (cooperative) branch of bistable solutions at weak incident driving  $\mathcal{R}_{\text{eff}} \simeq \mathcal{R}/(2C+1)$  [41], and assuming  $\tilde{\gamma} \gg \mathcal{R}, \tilde{\Omega}$ , we derive  $n_c \simeq 2N\mathcal{R}^2/\tilde{\gamma}$ . Numerically, for different incident fields and lattice constants, we typically find an intensity scaling of  $\propto N^{1+\alpha}$  where  $\alpha$  is a small positive or negative number  $0.1 \lesssim |\alpha| \lesssim 0.4$ . An analogous formula applies for incoherent scattering, with the necessary adjustments in the correlation functions (Appendix A). For the upper (single-atom) branch of bistable solutions at high intensities, the single-atom incoherent scattering dominates as  $\mathcal{R}_{\text{eff}} \simeq \mathcal{R}$  [41], resulting in the intensity being proportional to  $N$ . In the case of CRF from Eq. (10), the two-atom quantum correlations become significant, with the asymptotic scaling of the scattered intensity again  $\propto N\tilde{\gamma}/\gamma$ , diverging from the noninteracting result  $\propto N^2$  [32, 33].

### III. CONCLUDING REMARKS

We have demonstrated how DD interactions can lead to pronounced behaviors of saturation and effective driving field curves, phase transitions, and significant quantum fluctuations beyond the mean-field theory. Contrary to the gradual change observed in the second-order phase transition, where the sharp transition point is reached as  $N \rightarrow \infty$ , the discontinuous first-order transition occurs at a finite critical  $N$ . A full quantum treatment would also affect the first-order phase transition. It is generally well understood that bistable behavior coincides with enhanced quantum fluctuations [39, 40, 46, 55, 63–67], resulting in bimodal quantum distributions that represent tunnelling between the two mean-field solutions.

Historically, the CRF phase transition has been regarded as a highly idealized theoretical model, posing significant experimental challenges. Ideally, every atom should experience the same field exposure and no interactions, any deviation from which could severely limit the coherence time of the decay. These conclusions also align with the recent theoretical studies parallel to ours [42, 43]. Our interacting lattice scheme faces similar challenges, although we discovered that strong DD

interactions in regular arrays can enhance the necessary indistinguishability of the atoms through delocalization of excitations. In practical experiments, the atoms in the array should be prepared close to the steady states of the CRF model, achievable by modulating field, atom, or lattice parameters. For instance, the state  $s_- = i\beta$ ,  $s_z = -\sqrt{s^2 - \beta^2}$  could be prepared from another driven pure steady state by adjusting the driving amplitude.

### ACKNOWLEDGMENTS

We acknowledge financial support from the UK EP-SRC Grant No. EP/S002952/1.

#### Appendix A: Scattered intensity and transmission

In atomic arrays, collective behavior can be observed in light transmission experiments [8, 10]. For large atomic layers, coherent light transmission and reflection of a plane wave demonstrate behavior similar to that in 1D electrodynamics for light [68]. The amplitude of coherently scattered light amplitude from a square array of uniformly excited atoms propagates as a collimated wave. In the limit of an infinite array, the scattered field, with the density of dipoles  $\mathcal{D}/a^2$  in a phase-uniform excitation, almost perfectly emulates a plane wave [44]

$$\epsilon_0 \langle \hat{\mathbf{E}}_s^+(x) \rangle = \frac{ik\hat{\mathbf{e}}_d \mathcal{D}}{2a^2} \rho_{ge} e^{ik|x|}, \quad (A1)$$

assuming the normal to the lattice aligns with the  $x$ -axis. The resonance linewidth of the corresponding uniform collective LLI eigenmode derives from the imaginary part of the 1D dipole radiation kernel [44]

$$\begin{aligned} v &= \gamma + \tilde{\gamma} = \gamma + \xi \sum_{\ell \neq j} \text{Im} \left[ \mathbf{G}_{dd}^{(j\ell)} \right] \\ &= \frac{\xi}{2a^2} \lim_{x \rightarrow 0} \text{Im} [ike^{ik|x|}] = \frac{3\pi\gamma}{k^2 a^2}. \end{aligned} \quad (A2)$$

Combining these two expressions yields the coherent transmission and reflection amplitude coefficients:

$$t = \frac{\int_{x>0} \hat{\mathbf{e}}_d \cdot \langle \hat{\mathbf{E}}^+(x) \rangle d\Omega}{\int_{x>0} \hat{\mathbf{e}}_d \cdot \mathcal{E}^+(\mathbf{r}) d\Omega}, \quad r = \frac{\int_{x<0} \hat{\mathbf{e}}_d \cdot \langle \hat{\mathbf{E}}_s^+(x) \rangle d\Omega}{\int_{x>0} \hat{\mathbf{e}}_d \cdot \mathcal{E}^+(\mathbf{r}) d\Omega}, \quad (A3)$$

where  $t = 1 + r$  due to the symmetry, and we obtain

$$r = i(\gamma + \tilde{\gamma}) \frac{\rho_{ge}}{\mathcal{R}}. \quad (A4)$$

Here  $\rho_{ge}$  can be evaluated from Eq. (4a).

We express the total scattered intensity as a photon scattering rate over a surface  $S$  that completely encloses the atoms. The rate is given by the integral of the scattered intensity per photon energy

$$n_s = \frac{1}{\hbar\omega} \int_S dSI_s = \frac{2\epsilon_0 c}{\hbar\omega} \int_S dS \langle \hat{\mathbf{E}}_s^-(\mathbf{r}) \cdot \hat{\mathbf{E}}_s^+(\mathbf{r}) \rangle. \quad (A5)$$

The general expression can be evaluated [44, 69]:

$$n_s = 2\gamma \sum_j \langle \hat{\sigma}_j^+ \hat{\sigma}_j^- \rangle + 2\xi \sum_{j\ell (j \neq \ell)} \text{Im}[G_{dd}^{(j\ell)}] \langle \hat{\sigma}_j^+ \hat{\sigma}_\ell^- \rangle. \quad (\text{A6})$$

The coherent scattering rate Eq. (11) is obtained by factorizing all terms  $\langle \hat{\sigma}_j^+ \hat{\sigma}_\ell^- \rangle \rightarrow \langle \hat{\sigma}_j^+ \rangle \langle \hat{\sigma}_\ell^- \rangle$ . This is straightforward to calculate for the phase-uniform mode and yields Eq. (12), since  $\langle \hat{\sigma}_j^\pm \rangle$  can be factored out of the sum. The incoherently scattered light includes both single-atom and many-atom contributions. Single-atom contributions are derived from  $\langle \hat{\sigma}_j^+ \hat{\sigma}_j^- \rangle - \langle \hat{\sigma}_j^+ \rangle \langle \hat{\sigma}_j^- \rangle$ . For the

phase-uniform state, these yield

$$n_{\text{inc}}^{(1)} = 2N\gamma(\rho_{ee} - |\rho_{ge}|^2). \quad (\text{A7})$$

On the other hand, the many-atom contributions are given by

$$n_{\text{inc}}^{(2)} = 2N(\gamma + \tilde{\gamma})(\langle \hat{\sigma}_j^+ \hat{\sigma}_\ell^- \rangle - \langle \hat{\sigma}_j^+ \rangle \langle \hat{\sigma}_\ell^- \rangle), \quad j \neq \ell. \quad (\text{A8})$$

The leading order  $N$  dependence in the front of the expression is now  $\propto N\tilde{\gamma}/\gamma$  [see Fig. 2(a)], instead of the characteristic  $\propto N$  or  $\propto N^2$ . For fixed atomic positions, Eq. (A8) signifies many-atom quantum effects. However, if atomic positions fluctuate, the corresponding expression can also contain significant classical contributions [44, 45].

- 
- [1] H. Bender, C. Stehle, S. Slama, R. Kaiser, N. Piovella, C. Zimmermann, and P. W. Courteille, Observation of cooperative mie scattering from an ultracold atomic cloud, *Phys. Rev. A* **82**, 011404(R) (2010).
- [2] S. Balik, A. L. Win, M. D. Havey, I. M. Sokolov, and D. V. Kupriyanov, Near-resonance light scattering from a high-density ultracold atomic  $^{87}\text{Rb}$  gas, *Phys. Rev. A* **87**, 053817 (2013).
- [3] J. Pellegrino, R. Bourgain, S. Jennewein, Y. R. P. Sortais, A. Browaeys, S. D. Jenkins, and J. Ruostekoski, Observation of suppression of light scattering induced by dipole-dipole interactions in a cold-atom ensemble, *Phys. Rev. Lett.* **113**, 133602 (2014).
- [4] S. D. Jenkins, J. Ruostekoski, J. Javanainen, R. Bourgain, S. Jennewein, Y. R. P. Sortais, and A. Browaeys, Optical resonance shifts in the fluorescence of thermal and cold atomic gases, *Phys. Rev. Lett.* **116**, 183601 (2016).
- [5] S. Jennewein, M. Besbes, N. J. Schilder, S. D. Jenkins, C. Sauvan, J. Ruostekoski, J.-J. Greffet, Y. R. P. Sortais, and A. Browaeys, Coherent scattering of near-resonant light by a dense microscopic cold atomic cloud, *Phys. Rev. Lett.* **116**, 233601 (2016).
- [6] L. Corman, J. L. Ville, R. Saint-Jalm, M. Aidelsburger, T. Bienaimé, S. Nascimbène, J. Dalibard, and J. Beugnon, Transmission of near-resonant light through a dense slab of cold atoms, *Phys. Rev. A* **96**, 053629 (2017).
- [7] R. Saint-Jalm, M. Aidelsburger, J. L. Ville, L. Corman, Z. Hadzibabic, D. Delande, S. Nascimbène, N. Cherroret, J. Dalibard, and J. Beugnon, Resonant-light diffusion in a disordered atomic layer, *Phys. Rev. A* **97**, 061801 (2018).
- [8] J. Rui, D. Wei, A. Rubio-Abadal, S. Hollerith, J. Zeiher, D. M. Stamper-Kurn, C. Gross, and I. Bloch, A subradiant optical mirror formed by a single structured atomic layer, *Nature* **583**, 369 (2020).
- [9] G. Ferioli, A. Glicenstein, L. Henriët, I. Ferrier-Barbut, and A. Browaeys, Storage and release of subradiant excitations in a dense atomic cloud, *Phys. Rev. X* **11**, 021031 (2021).
- [10] K. Srakaew, P. Weckesser, S. Hollerith, D. Wei, D. Adler, I. Bloch, and J. Zeiher, A subwavelength atomic array switched by a single rydberg atom, *Nature Physics* **19**, 714 (2023).
- [11] R. H. Dicke, Coherence in spontaneous radiation processes, *Phys. Rev.* **93**, 99 (1954).
- [12] A. A. Svidzinsky, J.-T. Chang, and M. O. Scully, Dynamical evolution of correlated spontaneous emission of a single photon from a uniformly excited cloud of  $n$  atoms, *Phys. Rev. Lett.* **100**, 160504 (2008).
- [13] C. C. Kwong, T. Yang, M. S. Pramod, K. Pandey, D. Delande, R. Pierrat, and D. Wilkowski, Cooperative emission of a coherent superflash of light, *Phys. Rev. Lett.* **113**, 223601 (2014).
- [14] M. O. Araújo, I. Krešić, R. Kaiser, and W. Guerin, Superradiance in a large and dilute cloud of cold atoms in the linear-optics regime, *Phys. Rev. Lett.* **117**, 073002 (2016).
- [15] S. J. Roof, K. J. Kemp, M. D. Havey, and I. M. Sokolov, Observation of single-photon superradiance and the cooperative lamb shift in an extended sample of cold atoms, *Phys. Rev. Lett.* **117**, 073003 (2016).
- [16] P. Solano, P. Barberis-Blostein, F. K. Fatemi, L. A. Orozco, and S. L. Rolston, Super-radiance reveals infinite-range dipole interactions through a nanofiber, *Nature Communications* **8**, 1857 (2017).
- [17] R. T. Sutherland and F. Robicheaux, Superradiance in inverted multilevel atomic clouds, *Phys. Rev. A* **95**, 033839 (2017).
- [18] S. Okaba, D. Yu, L. Vincetti, F. Benabid, and H. Katori, Superradiance from lattice-confined atoms inside hollow core fibre, *Communications Physics* **2**, 136 (2019).
- [19] F. Robicheaux, Theoretical study of early-time superradiance for atom clouds and arrays, *Phys. Rev. A* **104**, 063706 (2021).
- [20] A. Piñeiro Orioli, J. K. Thompson, and A. M. Rey, Emergent dark states from superradiant dynamics in multi-level atoms in a cavity, *Phys. Rev. X* **12**, 011054 (2022).
- [21] S. J. Masson and A. Asenjo-García, Universality of dicke superradiance in arrays of quantum emitters, *Nature Communications* **13**, 2285 (2022).
- [22] S. Asselie, A. Cipris, and W. Guerin, Optical interpretation of linear-optics superradiance and subradiance, *Phys. Rev. A* **106**, 063712 (2022).

- [23] D. Malz, R. Trivedi, and J. I. Cirac, Large- $n$  limit of dicker superradiance, *Phys. Rev. A* **106**, 013716 (2022).
- [24] O. Rubies-Bigorda, S. Ostermann, and S. F. Yelin, Characterizing superradiant dynamics in atomic arrays via a cumulant expansion approach, *Phys. Rev. Res.* **5**, 013091 (2023).
- [25] C. Liedl, F. Tebbenjohanns, C. Bach, S. Pucher, A. Rauschenbeutel, and P. Schneeweiss, Observation of superradiant bursts in a cascaded quantum system, *Phys. Rev. X* **14**, 011020 (2024).
- [26] I. R. Senitzky, Interaction between a nonlinear oscillator and a radiation field, *Phys. Rev. A* **6**, 1175 (1972).
- [27] G. S. Agarwal, A. C. Brown, L. M. Narducci, and G. Vetri, Collective atomic effects in resonance fluorescence, *Phys. Rev. A* **15**, 1613 (1977).
- [28] P. Drummond and H. Carmichael, Volterra cycles and the cooperative fluorescence critical point, *Optics Communications* **27**, 160 (1978).
- [29] D. F. Walls, P. D. Drummond, S. S. Hassan, and H. J. Carmichael, Non-Equilibrium Phase Transitions in Cooperative Atomic Systems, *Progress of Theoretical Physics Supplement* **64**, 307 (1978).
- [30] L. M. Narducci, D. H. Feng, R. Gilmore, and G. S. Agarwal, Transient and steady-state behavior of collective atomic systems driven by a classical field, *Phys. Rev. A* **18**, 1571 (1978).
- [31] R. Puri and S. Lawande, Exact steady-state density operator for a collective atomic system in an external field, *Physics Letters A* **72**, 200 (1979).
- [32] H. J. Carmichael, Analytical and numerical results for the steady state in cooperative resonance fluorescence, *Journal of Physics B: Atomic and Molecular Physics* **13**, 3551 (1980).
- [33] P. D. Drummond, Observables and moments of cooperative resonance fluorescence, *Phys. Rev. A* **22**, 1179 (1980).
- [34] G. Ferioli, A. Glicenstein, I. Ferrier-Barbut, and A. Browaeys, A non-equilibrium superradiant phase transition in free space, *Nature Physics* **19**, 1345 (2023).
- [35] R. Bonifacio and L. Lugiato, Cooperative effects and bistability for resonance fluorescence, *Optics Communications* **19**, 172 (1976).
- [36] R. Bonifacio and L. A. Lugiato, Optical bistability and cooperative effects in resonance fluorescence, *Phys. Rev. A* **18**, 1129 (1978).
- [37] H. J. Carmichael and D. F. Walls, Hysteresis in the spectrum for cooperative resonance fluorescence, *Journal of Physics B: Atomic and Molecular Physics* **10**, L685 (1977).
- [38] G. P. Agrawal and H. J. Carmichael, Optical bistability through nonlinear dispersion and absorption, *Phys. Rev. A* **19**, 2074 (1979).
- [39] P. D. Drummond and D. F. Walls, Quantum theory of optical bistability. I. Nonlinear polarisability model, *Journal of Physics A: Mathematical and General* **13**, 725 (1980).
- [40] P. D. Drummond and D. F. Walls, Quantum theory of optical bistability. II. Atomic fluorescence in a high- $Q$  cavity, *Phys. Rev. A* **23**, 2563 (1981).
- [41] C. D. Parmee and J. Ruostekoski, Bistable optical transmission through arrays of atoms in free space, *Phys. Rev. A* **103**, 033706 (2021).
- [42] S. Agarwal, E. Chaparro, D. Barberena, A. P. Orioli, G. Ferioli, S. Pancaldi, I. Ferrier-Barbut, A. Browaeys, and A. M. Rey, Directional superradiance in a driven ultracold atomic gas in free-space (2024), [arXiv:2403.15556](https://arxiv.org/abs/2403.15556) [[cond-mat.quant-gas](https://arxiv.org/abs/2403.15556)].
- [43] D. Goncalves, L. Bombieri, G. Ferioli, S. Pancaldi, I. Ferrier-Barbut, A. Browaeys, E. Shahmoon, and D. E. Chang, Driven-dissipative phase separation in free-space atomic ensembles (2024), [arXiv:2403.15237](https://arxiv.org/abs/2403.15237) [[quant-ph](https://arxiv.org/abs/2403.15237)].
- [44] J. Ruostekoski, Cooperative quantum-optical planar arrays of atoms, *Phys. Rev. A* **108**, 030101 (2023).
- [45] R. J. Bettles, M. D. Lee, S. A. Gardiner, and J. Ruostekoski, Quantum and nonlinear effects in light transmitted through planar atomic arrays, *Commun. Phys.* **3**, 141 (2020).
- [46] C. D. Parmee and J. Ruostekoski, Signatures of optical phase transitions in superradiant and subradiant atomic arrays, *Commun. Phys.* **3**, 205 (2020).
- [47] J. D. Jackson, *Classical Electrodynamics*, 3rd ed. (Wiley, New York, 1999).
- [48] G. Facchinetti, S. D. Jenkins, and J. Ruostekoski, Storing light with subradiant correlations in arrays of atoms, *Phys. Rev. Lett.* **117**, 243601 (2016).
- [49] M. T. Manzoni, M. Moreno-Cardoner, A. Asenjo-Garcia, J. V. Porto, A. V. Gorshkov, and D. E. Chang, Optimization of photon storage fidelity in ordered atomic arrays, *New J. Phys.* **20**, 083048 (2018).
- [50] J. Ruostekoski and J. Javanainen, Quantum field theory of cooperative atom response: Low light intensity, *Phys. Rev. A* **55**, 513 (1997).
- [51] M. Rusek, A. Orłowski, and J. Mostowski, Localization of light in three-dimensional random dielectric media, *Phys. Rev. E* **53**, 4122 (1996).
- [52] S. D. Jenkins, J. Ruostekoski, J. Javanainen, S. Jennewein, R. Bourgain, J. Pellegrino, Y. R. P. Sortais, and A. Browaeys, Collective resonance fluorescence in small and dense atom clouds: Comparison between theory and experiment, *Phys. Rev. A* **94**, 023842 (2016).
- [53] T. E. Lee, H. Häffner, and M. C. Cross, Antiferromagnetic phase transition in a nonequilibrium lattice of Rydberg atoms, *Phys. Rev. A* **84**, 031402 (2011).
- [54] N. Šibalić, C. G. Wade, C. S. Adams, K. J. Weatherill, and T. Pohl, Driven-dissipative many-body systems with mixed power-law interactions: Bistabilities and temperature-driven nonequilibrium phase transitions, *Phys. Rev. A* **94**, 011401 (2016).
- [55] C. D. Parmee and N. R. Cooper, Phases of driven two-level systems with nonlocal dissipation, *Phys. Rev. A* **97**, 053616 (2018).
- [56] C. Carr, R. Ritter, C. G. Wade, C. S. Adams, and K. J. Weatherill, Nonequilibrium Phase Transition in a Dilute Rydberg Ensemble, *Phys. Rev. Lett.* **111**, 113901 (2013).
- [57] B. Olmos, D. Yu, Y. Singh, F. Schreck, K. Bongs, and I. Lesanovsky, Long-range interacting many-body systems with alkaline-earth-metal atoms, *Phys. Rev. Lett.* **110**, 143602 (2013).
- [58] K. E. Ballantine, D. Wilkowski, and J. Ruostekoski, Optical magnetism and wavefront control by arrays of strontium atoms, *Phys. Rev. Res.* **4**, 033242 (2022).
- [59] K. Beloy, J. A. Sherman, N. D. Lemke, N. Hinkley, C. W. Oates, and A. D. Ludlow, Determination of the  $5d6s\ ^3D_1$  state lifetime and blackbody-radiation clock shift in yb, *Phys. Rev. A* **86**, 051404 (2012).
- [60] S. D. Jenkins and J. Ruostekoski, Controlled manipulation of light by cooperative response of atoms in an optical lattice, *Phys. Rev. A* **86**, 031602 (2012).

- [61] O. Morsch and M. Oberthaler, Dynamics of bose-einstein condensates in optical lattices, *Rev. Mod. Phys.* **78**, 179 (2006).
- [62] J. Hannukainen and J. Larson, Dissipation-driven quantum phase transitions and symmetry breaking, *Phys. Rev. A* **98**, 042113 (2018).
- [63] H. Carmichael, "Theory of Quantum Fluctuations in Optical Bistability", in *Front. Quantum Opt.* (Adam Hilger, Bristol, 1986) pp. 120–203.
- [64] B. Olmos, D. Yu, and I. Lesanovsky, Steady-state properties of a driven atomic ensemble with nonlocal dissipation, *Phys. Rev. A* **89**, 023616 (2014).
- [65] G. Rempe, R. J. Thompson, R. J. Brecha, W. D. Lee, and H. J. Kimble, Optical bistability and photon statistics in cavity quantum electrodynamics, *Phys. Rev. Lett.* **67**, 1727 (1991).
- [66] H. Alaeian and B. Buča, Exact multistability and dissipative time crystals in interacting fermionic lattices, *Communications Physics* **5**, 318 (2022).
- [67] N. Leppenen and E. Shahmoon, Quantum bistability at the interplay between collective and individual decay (2024), [arXiv:2404.02134 \[quant-ph\]](https://arxiv.org/abs/2404.02134).
- [68] J. Javanainen and R. Rajapakse, Light propagation in systems involving two-dimensional atomic lattices, *Phys. Rev. A* **100**, 013616 (2019).
- [69] H. Carmichael and K. Kim, A quantum trajectory unraveling of the superradiance master equation, *Opt. Commun.* **179**, 417 (2000).